ORIGINAL RESEARCH

MR Spectroscopic Imaging of Peripheral Zone in Prostate Cancer Using a 3T MRI Scanner: Endorectal versus External Phased Array Coils

Rajakumar Nagarajan[1], Daniel JA Margolis[1], Steven S. Raman[1], David Ouellette[1], Manoj K. Sarma[1], Robert E. Reiter[2] and M. Albert Thomas[1]

[1]Radiological Sciences, University of California Los Angeles, Los Angeles, CA, USA. [2]Urology, University of California Los Angeles, Los Angeles, CA, USA. Corresponding author email: athomas@mednet.ucla.edu

Abstract: Magnetic resonance spectroscopic imaging (MRSI) detects alterations in major prostate metabolites, such as citrate (Cit), creatine (Cr), and choline (Ch). We evaluated the sensitivity and accuracy of three-dimensional MRSI of prostate using an endorectal compared to an external phased array "receive" coil on a 3T MRI scanner. Eighteen patients with prostate cancer (PCa) who underwent endorectal MR imaging and proton (1H) MRSI were included in this study. Immediately after the endorectal MRSI scan, the PCa patients were scanned with the external phased array coil. The endorectal coil-detected metabolite ratio [(Ch+Cr)/Cit] was significantly higher in cancer locations (1.667 ± 0.663) compared to non-cancer locations (0.978 ± 0.420) ($P < 0.001$). Similarly, for the external phased array, the ratio was significantly higher in cancer locations (1.070 ± 0.525) compared to non-cancer locations (0.521 ± 0.310) ($P < 0.001$). The sensitivity and accuracy of cancer detection were 81% and 78% using the endorectal 'receive' coil, and 69% and 75%, respectively using the external phased array 'receive' coil.

Keywords: prostate cancer, MRSI, metabolites, external coil, sensitivity, citrate, choline, creatine

This article is available from http://www.la-press.com.

Introduction

Prostate cancer (PCa) is the most common non-cutaneous cancer and second leading cause of cancer death in men. In 2012, approximately 241,740 new cases and 28,170 PCa-related deaths occurred in the United States.[1] Magnetic resonance imaging (MRI) has been used to evaluate prostate anatomy and prostate pathologies for several years. MRI, with its excellent soft-tissue differentiation, provides high-resolution images of the prostate and surrounding structures. Magnetic resonance spectroscopy (MRS) is a powerful tool for exploring the cellular chemistry of human tissues.[2–6] There is a growing body of evidence that proton MRS can be used for clinical evaluation of PCa and metabolic alterations before and after therapy. Magnetic resonance spectroscopic imaging (MRSI) can be used to measure metabolite levels in the tissue, particularly choline (Ch), citrate (Cit), creatine (Cr), and various polyamines (spermine, spermidine, and putrecine). PCa typically shows an increased concentration of Ch and reduction of Cit and polyamines.

MRSI of the prostate is typically performed using a combination of point-resolved spectroscopy (PRESS)[7] and three-dimensional localized MRSI[8] rather than the traditional single-voxel or slice-based two-dimensional MRSI technique was used in brain spectroscopic imaging. 3D MRSI requires phase encoding along the three spatial dimensions, conventionally known as frequency, phase, and slice. Acquisition time and coverage of the prostate are the primary considerations in choosing matrix dimensions. Acquiring 3D MRSI data with higher spatial resolution requires a long total acquisition time. Conventional prostate MRSI studies involving average weighted encoding use a long echo time (TE) with a short repetition time (TR), allowing observation of a reduced number of metabolites.[9] Long TEs are used for 3D MRSI due to the addition of MEGA[10] radio-frequency pulses for both water and lipid suppression. The interpretation system most used to discriminate between cancer and normal prostatic tissue in the peripheral zone was described by Kurhanewicz et al.[9] They calculated the peak area ratios of Ch and Cr to Cit [(Ch+Cr)/Cit] for each voxel. Inclusion of Cr in this ratio is mandatory because of the Cr peak is very close to the Ch peak in the spectrum. However, Cr appears be maintained at a relatively constant level in both healthy and tumor prostatic tissues.

It was unknown whether the quality of endorectal MRSI scanning could be improved by using a stronger (3T) scanner and/or using perfluorocarbon (PFC) in the endorectal coil (ERC) instead of air. Rather than filling air, PFC has been shown to improve MRSI image quality and the magnetic susceptibility closely matching that of prostate.[11] The ERC is contraindicated in a number of patients (eg, after abdominal perineal resection for rectal cancers or after radiation therapy for the pelvis).[12] In some cases, it is preferable to not use an ERC to avoid structural deformation of the prostate peripheral zone, which is often compressed by an ERC. The ERC also causes signal hyperintensity near the rectum and the neighboring peripheral zone. Signal hyperintensity and tissue deformation can make complicate diagnostic interpretation. Previous studies have reported the use of external phased array coils for prostate MR spectroscopy in 3T.[13–20] The major goal of the study was to evaluate 3T MRSI for the peripheral zone in prostate cancer patients using an endorectal coil and to compare the performance of 3T MRSI and an external phased array 'receive' coil.

Materials and Methods

Eighteen patients ranging in age from 56–72 years (mean, 63.1 years) with PCa who underwent endorectal MR imaging and proton MR spectroscopic imaging were included in this study. The study protocol was approved by the Institutional Review Board, and informed consent was obtained from each patient. Gleason scores for the tumor on prostate biopsy ranged from 3 to 8, while prostate-specific antigen varied from 2.8 to 20.6 ng/mL (mean of 6.84 ng/mL). A Siemens 3T MRI Scanner with high-performance gradients (Trio-Tim, Siemens Medical Solutions, Erlangen, Germany) was used in this investigation. A quadrature body 'transmit' coil was used to transmit radio-frequency pulses. An endorectal inflatable 'receive' coil (Medrad Corporation, Indianola, PA, USA) was then inserted into the rectum and inflated with 50 cc PFC. The coil was positioned horizontally at approximately the 10:00 and 2:00 positions. After endorectal scanning, patients were scanned with the external phased array 'receive' coil for the comparison study. T_2-weighted images in the transverse, sagittal, and coronal planes were acquired by using a turbo spin-echo sequence. The MRI protocol included

T_2-weighted images acquired using a fast spin-echo sequence with: repetition time (TR) = 3,800 ms, effective echo time (TE) = 101 ms, slice thickness = 3 mm, field of view = 140 mm, and matrix size = 256×256 mm². MRSI was performed in all patients, which included a 3D water- and fat-suppressed spectroscopic acquisition. 3D MRSI parameters of the endorectal and external phased array coil were as follows: TR 750 ms, TE 145 ms, acquisition bandwidth 1250 Hz, 6 averages, and 512 spectral data points with a voxel resolution of 0.3 mL. Total acquisition time was approximately 12 min. For the external phased array, the voxel resolution was 0.35 mL. A PRESS-based sequence was used to acquire proton MR spectra from a volume of interest (VOI) of approximately $55 \times 45 \times 45$ mm³. Outer volume suppression of water and lipid was achieved using eight 3-cm thick saturation pulses around the VOI.

A spectroscopist examined the MRSI data set and reported the location and number of suspicious voxels to the radiologist, to identify metabolite ratios predictive of cancer. For 3D MRSI post-processing, each spectrum was Fourier transformed, frequency-, phase-, and baseline-corrected, and the peaks of Cit, Ch, and Cr were subsequently fitted. A Hamming filter was used for the MRSI spatial dimensions of the data. For tumor localization, the prostate was split along the midline and further divided into the apex, the middle, and the base of the gland. According to histopathologic findings, the voxels and corresponding spectra were assigned as normal tissue or tumor tissue. For selected voxels in the peripheral zone, the area under the curve of the metabolite resonances was determined and the signal intensity ratio for (Ch+Cr)/Cit was calculated using commercially available software from Siemens. Peak areas for Ch, Cr, Spm, and Cit were calculated using numeric integration. Metabolic maps of (Ch+Cr)/Cit were generated since Spm cannot be separated from Ch and Cr peaks. Voxels were considered suitable if they consisted of at least 75% peripheral zone tissue and did not include periurethral tissue. If the Cit peak was lower than the Ch peak or was undetectable, the voxel was determined to be malignant. If the Cit peak was higher than the Ch peak, the voxel was considered noncancerous for (Ch+Cr)/Cit values smaller than 0.50 and malignant for (Ch+Cr)/Cit values greater than 0.50.

For the external phased array coil, the noncancerous ratio was less than 0.28 and the malignant ratio was greater than 0.28.

The paired t-test was used to determine whether the ratios of (Ch+Cr)/Cit in cancer were different from those in non-cancer using an endorectal coil and external coil. A P-value less than 0.05 was considered statistically significant.

Receiver operating characteristic (ROC) curve analyses based on logistic regression models were performed to identify the optimal cutoff value for predicting metabolite ratios using the endorectal coil and external phased array coil. The area under the curve (AUC), interpreted as the average value of sensitivity for all possible values of specificity, was used in the ROC analysis. An area of 0.50 implies that the variable adds no information, whereas an area of 1 implies perfect accuracy. Sensitivity, specificity, positive predictive value (PPV), and negative predictive value (NPV) as well as accuracy were reported for the optimal thresholds. P-values < 0.05 were considered statistically significant. Statistical analyses were performed using SPSS software (Statistical Package for the Social Sciences, Version 18.0, SPSS Inc, Chicago, IL, USA).

Results

Figure 1A and B show the metabolite ratios (Ch+Cr)/Cit for cancer and non-cancer locations with endorectal and external phased array coil in 18 PCa patients. For the endorectal coil, the metabolite ratio (mean ± SD) was significantly higher in cancer locations (1.667 ± 0.663) compared to in non-cancer locations (0.978 ± 0.420) ($P < 0.001$). Similarly, for the external phased array coil, the ratio was significantly higher in cancer locations (1.070 ± 0.525) than in non-cancer locations (0.521 ± 0.310) ($P < 0.001$). Figure 2A and B show a comparison of endorectal and external phased array MR Spectroscopic Imaging of a 67 year-old PCa patient. A significant elevation in Ch/Cr and decreased Cit were observed in the right side peripheral zone of the PCa patient scanned using endorectal coil. Similar trends for metabolite changes are shown in Figure 2B with a slightly worse signal-to-noise ratio (SNR) because the patient was scanned using an external coil. Table 1 shows the full width at half maximum (FWHM) of Cit and (Cr+Ch) in cancer and noncancerous locations using the
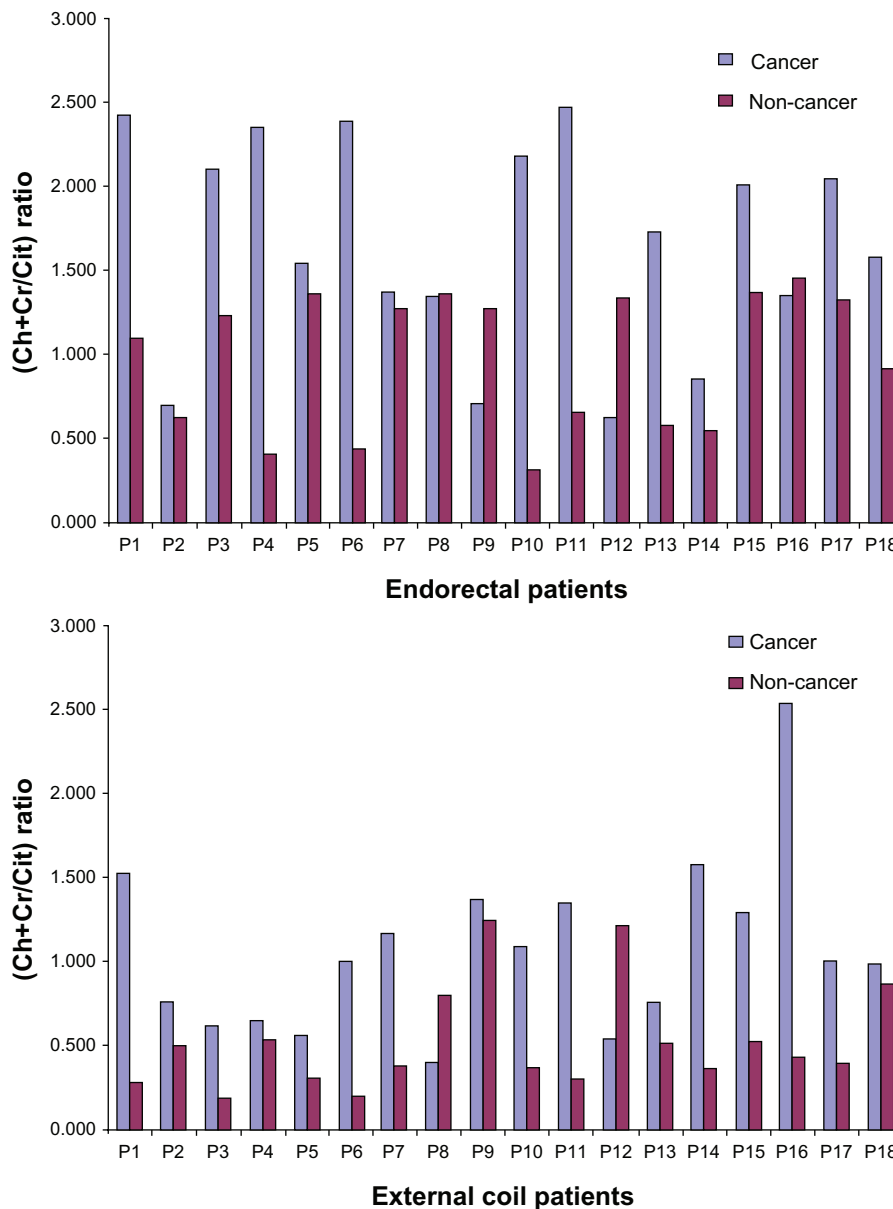
Figure 1. Comparison of metabolite ratios [(Ch+Cr)/Cit] in 18 PCa patients scanned with the endorectal and external body array 'receive' coils.
Note: Significant (*P* < 0.05) elevation of Ch/Cr observed in cancer locations compared to non-cancer locations in both coils.

endorectal and external phased array coil. The mean FWHM of Cit in cancer and non-cancer locations for patients scanned using the endorectal coil were 11.7 and 11.5 Hz respectively, whereas using the external coil, the mean FWHM values were 17.7 and 19.5 Hz, which showed a higher coefficient of variance (CV). Similarly, the mean FWHM of Ch+Cr in cancer and non-cancer locations of patients scanned using the endorectal coil were 17.7 and 19.5 Hz, where in the external coil, the mean FWHM values were 25.7 and 28 Hz with a higher CV. The mean global water line width of 25 Hz observed using the endorectal coil and

31 Hz was observed using the external phased array coil with higher CV.

Figure 3 shows that the MRSI metabolite ratios in peripheral zone cancer locations derived from endorectal coil- and external body coil were positively and linearly correlated (R^2 = 0.571). Figure 4 shows the comparison of receiver operating characteristics curves for the endorectal coil- and external body coil-derived MRSI ratio. ROC curve analyses for differentiating endorectal coil suggested an optimal cutoff value of 1.35. This implies that the proportions of correctly identified endorectal coil sensitivity, specificity,
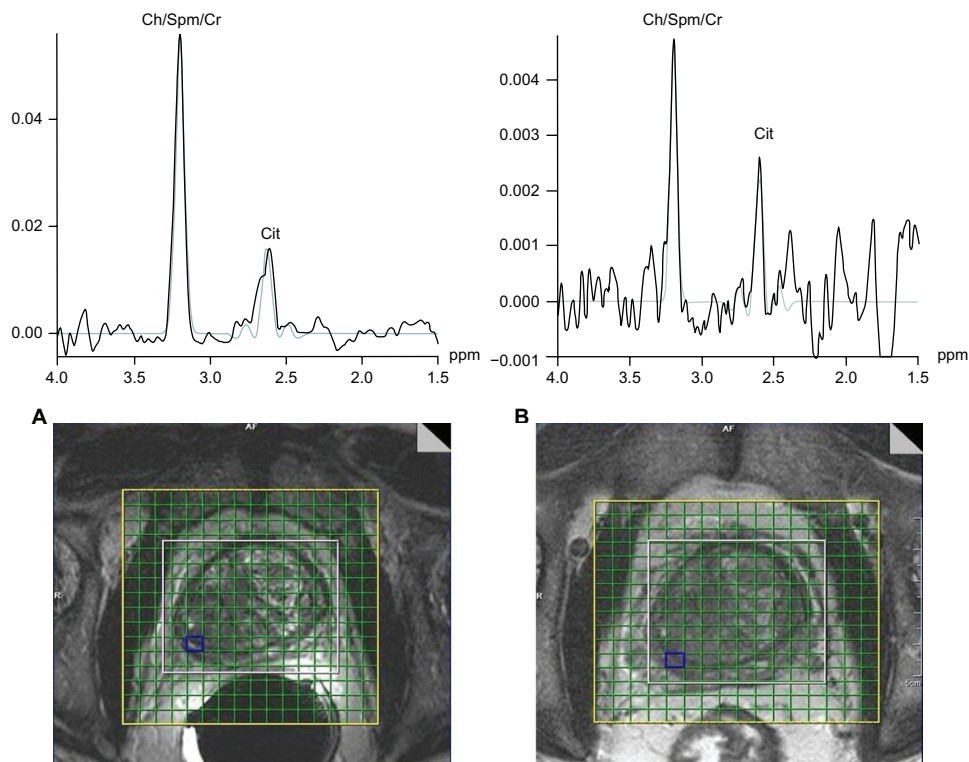
Figure 2. Comparison of (**A**) endorectal and (**B**) external body array MR Spectroscopic Imaging of a 67-year old PCa patient.
Note: Extracted single voxel spectra show a significant ($P < 0.05$) elevation of Ch/Cr and declined Cit in the right side peripheral zone of the PCa patient in both coils.

PPV, and NPV were 81.3%, 75.0%, 76.5%, and 80.0%, respectively. The AUC was 86.9%, with an accuracy of 78.1%. The cutoff value for the external body coil was 0.77 for sensitivity, specificity, and accuracy values of 68.8%, 81.3%, and 75.0%, respectively. The AUC of the MRSI ratio slightly increased for endorectal coil (86.9%) compared to external phased array coil (85.9%). In the evaluation of the endorectal coil versus external phased array coil, the MRSI ratios showed an accuracy of 78.1%, indicating good discrimination compared to external phased array of 75.0%. Detailed results of the ROC curve analyses are shown in Table 2, which shows the sensitivity, specificity, PPV, NPV, AUC, and accuracy of classifying endorectal coil and external body coil.

Discussion

Numerous studies have suggested that MRSI using an ERC is the most promising technique for detecting and staging of PCa. At more commonly available clinical field strengths of 1.5T, an ERC is necessary for obtaining a sufficiently high SNR with subsequent spatial resolution, allowing reliable cancer delineation in a clinically reasonable time frame. However, the

Table 1. FWHM of water and metabolite resonances using endorectal and external body array "receive" coils.

Peak	Endorectal FWHM Mean ± SD	CV (%)	External body array FWHM Mean ± SD	CV (%)
Cancer Cit	11.73 ± 2.75	23.41	15.45 ± 6.17	39.96
Cancer (Cr+Ch)	17.71 ± 6.78	27.57	25.75 ± 8.47	32.88
Non-cancer Cit	11.53 ± 1.73	15.02	18.83 ± 10.16	53.94
Non-cancer (Cr+Ch)	19.59 ± 6.83	27.77	28.06 ± 10.80	38.49
Water	25.00 ± 5.16	20.64	31.00 ± 9.62	31.05

Note: The FWHM of the water resonance represents global line width whereas the FWHM values of metabolites were derived from spectra extracted from selected locations.
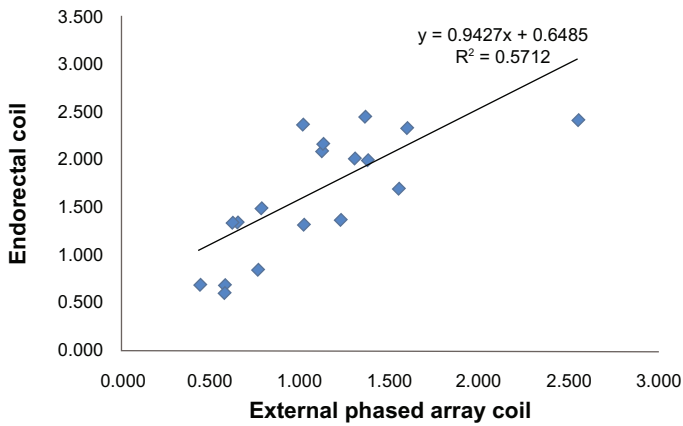
Figure 3. Correlation between the maximum ratios [(Ch+Cr)/Cit] of cancer identified in the peripheral zone with external phased array coil vs. endorectal coil MRS.
**Note:** A positive correlation was observed.

use of an ERC is more time-consuming, leading to higher costs and greater patient discomfort. Thus, we compared the performance of the endorectal coil with the external phased array coil at 3T.

Compared with external phased array coil at 3T, endorectal MR spectroscopy at 3T significantly improves spectral line width and coefficient of variance of metabolite ratio. The FWHM is a good indicator of spectral homogeneity. The FWHM value typically increases as VOI increases. Excellent quality of prostate spectra can be obtained through optimization of B_0 homogeneity for the PRESS-selected VOI. This procedure typically involves the combined use of a standard automatic shim provided by the manufacturer and, if necessary, manual adjustments of the linear x, y, and z gradients. Small improvements in shim can make a significant difference in spectra quality. Particularly, good B_0 homogeneity is essential

for sufficient water and lipid suppression. Water and lipid suppression is achieved through generation of frequency-selective MEGA pulses.[10] During MRSI acquisition, large lipid resonance peaks obscures the metabolite peak. Outer volume saturation pulses were used to eliminate signals from adjacent tissues, particularly periprostatic lipids and rectal wall tissue. The coefficient of variance was higher in the external phased array than for the endorectal coil due to the larger size of the coil and increased distance from the prostate proportional to abdominal circumference, leading to a decrease in the SNR ratio.

The overall accuracy of the external phased array coil MRSI has been shown to be slightly inferior to that using the endorectal coil in our pilot study involving a limited number of patients. In the localization of PCa with MRSI at 3T, the use of the endorectal coil showed a significantly ($P < 0.05$) higher sensitivity (81.3%) than the external phased array (68.8%). In contrast, the specificities of cancer detection were 81% and 75% using the external phased array and the endorectal coils, respectively. Additionally, there was a slight increase in the AUC (86.9%) for endorectal compared to the external phased array AUC (85.9%).

In our investigations using an external phased array coil, the effective voxel size was slightly larger to compensate for the poor SNR compared to examinations of the prostate using an endorectal coil. Overlap exists in the (Ch+Cr)/Cit ratios between cancer and noncancerous tissues. For both ERC and external phased array coils, (Ch+Cr)/Cit ratios were significantly higher in cancer locations than noncancer locations in this study, in accordance with the
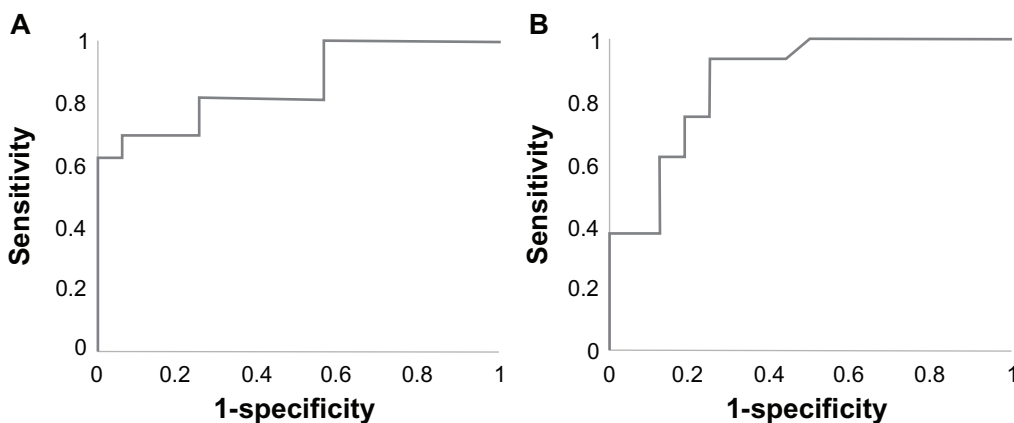
Figure 4. ROC curves of MRSI ratios of prostate cancer patients (**A**) with the endorectal and (**B**) the external phased array 'receive' coils.

Table 2. Measures of sensitivity, specificity, PPV, NPV, and accuracy of endorectal and external body coil MRSI ratios in discrimination of cancer from non-cancer with ROC curve analysis.

Parameter	Endorectal coil	External phased array
CV	1.35	0.77
Sensitivity, %	81.3	68.8
Specificity, %	75.0	81.3
PPV%	76.5	78.6
NPV%	80.0	72.2
AUC, %	86.9	85.9
Accuracy, %	78.1	75.0

Abbreviations: CV, cutoff value; PPV, positive predictive value; NPV, negative predictive value; AUC, area under the curve.

results of previous studies.[21–30] Additionally, the trend of accuracy and sensitivity of the ERC in this study agreed with that of a previous study.[20] The metabolite mean ratio of the external phased array coil was lower in cancer and non-cancer locations due to the low SNR. However, the ratio of (Ch+Cr)/Cit using both coils was generally positively and linearly correlated. Although AUC and sensitivity were elevated for ERC, the results imply that both ERC and external phased-array coil MRS are feasible for detecting the peripheral zone cancer with an optimal threshold ratio for (Ch+Cr)/Cit.

Although the sensitivity and accuracy increased in ERC, there are some disadvantages of using this method. Disadvantages of using an ERC include its invasiveness, image distortions, and a limited field of view. The accuracy of endorectal coil MRI is also frequently affected by image degradation. The three most common causes of this are near-field endorectal surface coil profile (because the coil is close to the gland), phase encoding artifact (from motion of feces or the rectum itself), and incorrect placement of the coil (where the coil is not parallel to the transverse plane of the gland).[31]

Another limitation is the small number of patients in this study. Additionally, there was no correlation between Gleason scores and MRSI ratios. Another limitation of this study was the inclusion of only the peripheral zone of the prostate, in which 75% cancer arises.

Conclusion

These preliminary findings confirmed that the use of ERC significantly improves spectral line width and the coefficient of variance of metabolite ratio compared with the external phased array coil. However, based on overall performance, use of the external phased array coil may be recommended for patients with rectal diseases or patients who could not tolerate the discomfort of endorectal surface coil insertion.

Author Contributions

Conceived and designed the experiments: RN, AT. Analysed the data: RN, DO, MS. Wrote the first draft of the manuscript: RN, AT. Contributed to the writing of the manuscript: DM, RR, SR. Agree with manuscript results and conclusions: RN, DM, SR, AT, MS. Jointly developed the structure and arguments for the paper: RN, AT. Made critical revisions and approved final version: RN, AT, DM, SR, AT. All authors reviewed and approved of the final manuscript.

Competing Interests

Author(s) disclose no potential conflicts of interest.

Disclosures and Ethics

As a requirement of publication author(s) have provided to the publisher signed confirmation of compliance with legal and ethical obligations including but not limited to the following: authorship and contributorship, conflicts of interest, privacy and confidentiality and (where applicable) protection of human and animal research subjects. The authors have read and confirmed their agreement with the ICMJE authorship and conflict of interest criteria. The authors have also confirmed that this article is unique and not under consideration or published in any other publication, and that they have permission from rights holders to reproduce any copyrighted material. Any disclosures

are made in this section. The external blind peer reviewers report no conflicts of interest. Provenance: the authors were invited to submit this paper.

References

1. American Cancer Society. Cancer Facts and Figures 2012. Atlanta, Ga: American Cancer Society; 2012. Availabe at: http://www.cancer.org/acs/groups/content/@epidemiologysurveilance/documents/document/acspc-031941.pdf.

2. Cornel EB, Smits GA, de Ruijter JE, et al. In vitro proton magnetic resonance spectroscopy of four human prostate cancer cell lines. *Prostate*. 1995(5);26:275–80.

3. Kurhanewicz J, Thomas A, Jajodia P, et al. 31P spectroscopy of the human prostate gland in vivo using a transrectal probe. *Magn Reson Med*. 1991;22(2):404–13.

4. Thomas MA, Narayan P, Kurhanewicz J, et al. Detection of phosphorus metabolites in human prostates with a transrectal 31P NMR probe. *J Magn Reson*. 1992;99:377–86.

5. Narayan P, Kurhanewicz J. Magnetic resonance spectroscopy in prostate disease: diagnostic possibilities and future developments. *Prostate Suppl*. 1992;Suppl 4:43–50.

6. van der Graaf M, Schipper RG, Oosterhof GO, Schalken JA, Verhofstad AA, Heerschap A. Proton MR spectroscopy of prostatic tissue focused on the detection of spermine, a possible biomarker of malignant behavior in prostate cancer. *MAGMA*. 2000;10(3):153–9.

7. Bottomley PA. Spatial localization in NMR spectroscopy in vivo. *Ann N Y Acad Sci*. 1987;508:333–48.

8. Brown TR, Kincaid BM, Ugurbil K. NMR chemical shift imaging in three dimensions. *Proc Natl Acad Sci U S A*. 1982;79(11):3523–6.

9. Kurhanewicz J, Vigneron DB, Hricak H, Narayan P, Carroll P, Nelson SJ. Three-dimensional H-1 MR spectroscopic imaging of the in situ human prostate with high (0.24–0.7-cm³) spatial resolution. *Radiology*. 1996;198(3):795–805.

10. Mescher M, Merkle H, Kirsch J, Garwood M, Gruetter R. Simultaneous in vivo spectral editing and water suppression. *NMR Biomed*. 1998;11(6):266–72.

11. Eilenberg SS, Tartar VM, Mattrey RF. Reducing magnetic susceptibility differences using liquid fluorocarbon pads (Sat Pad): results with spectral presaturation of fat. *Artif Cells Blood Substit Immobil Biotechnol*. 1994;22(4):1477–83.

12. Maio A, Rifkin MD. Magnetic resonance imaging of prostate cancer: update. *Top Magn Reson Imaging*. 1995;7(1):54–68.

13. Kim HW, Buckley DL, Peterson DM, et al. In vivo prostate magnetic resonance imaging and magnetic resonance spectroscopy at 3 Tesla using a transceive pelvic phased array coil: preliminary results. *Invest Radiol*. 2003;38(7):443–51.

14. Fütterer JJ, Scheenen TW, Huisman HJ, et al. Initial experience of 3 tesla endorectal coil magnetic resonance imaging and ¹H-spectroscopic imaging of the prostate. *Invest Radiol*. 2004;39(11):671–80.

15. Scheenen TW, Heijmink SW, Roell SA, et al. Three-dimensional proton MR spectroscopy of human prostate at 3T without endorectal coil: feasibility. *Radiology*. 2007;245(2):507–16.

16. Turkbey B, Mani H, Shah V, et al. Multiparametric 3T prostate magnetic resonance imaging to detect cancer: histopathological correlation using prostatectomy specimens processed in customized magnetic resonance imaging based molds. *J Urol*. 2011;186(5):1818–24.

17. Cornfeld DM, Weinreb JC. MR imaging of the prostate: 1.5T versus 3T. *Magn Reson Imaging Clin N Am*. 2007;15(3):433–48.

18. Turkbey B, Pinto PA, Mani H, et al. Prostate cancer: value of multiparametric MR imaging at 3T for detection—histopathologic correlation. *Radiology*. 2010;255(1):89–99.

19. Kim CK, Park BK, Park W, Kim SS. Prostate MR imaging at 3T using a phased-arrayed coil in predicting locally recurrent prostate cancer after radiation therapy: preliminary experience. *Abdom Imaging*. 2010;35(2):246–52.

20. Heijmink SW, Fütterer JJ, Hambrock T, et al. Prostate cancer: body-array versus endorectal coil MR imaging at 3T—comparison of image quality, localization, and staging performance. *Radiology*. 2007;244(1):184–95.

21. Yakar D, Heijmink SW, Hulsbergen-van de Kaa CA, et al. Initial results of 3-dimensional ¹H-magnetic resonance spectroscopic imaging in the localization of prostate cancer at 3 Tesla: should we use an endorectal coil? *Invest Radiol*. 2011;46(5):301–6.

22. Kaji Y, Wada A, Imaoka I, et al. Proton two-dimensional chemical shift imaging for evaluation of prostate cancer: external surface coil vs. endorectal surface coil. *J Magn Reson Imaging*. 2002;16(6);697–706.

23. Lichy MP, Pintaske J, Kottke R, et al. 3D proton MR spectroscopic imaging of prostate cancer using a standard spine coil at 1.5 T in clinical routine: a feasibility study. *Eur Radiol*. 2005;15(4):653–60.

24. Kim JK, Kim DY, Lee YH, et al. In vivo differential diagnosis of prostate cancer and benign prostatic hyperplasia: localized proton magnetic resonance spectroscopy using external-body surface coil. *Magn Reson Imaging*. 1998;16(10):1281–8.

25. Coakley FV, Kurhanewicz J, Lu Y, et al. Prostate cancer tumor volume: measurement with endorectal MR and MR spectroscopic imaging. *Radiology*. 2002;223(1):91–7.

26. Carlani M, Mancino S, Bonanno E, et al. Combined morphological, [¹H]-MR spectroscopic and contrast-enhanced imaging of human prostate cancer with a 3-Tesla scanner: preliminary experience. *Radiol Med*. 2008;113(5):670–88.

27. Kumar R, Kumar M, Jagannathan NR, Gupta NP, Hemal AK. Proton magnetic resonance spectroscopy with a body coil in the diagnosis of carcinoma prostate. *Urol Res*. 2004;32(1):36–40.

28. Scheidler J, Hricak H, Vigneron DB, et al. Prostate cancer: localization with three-dimensional proton MR spectroscopic imaging–clinicopathologic study. *Radiology*. 1999;213(2):473–80.

29. Shukla-Dave A, Hricak H, Kattan MW, et al. The utility of magnetic resonance imaging and spectroscopy for predicting insignificant prostate cancer: an initial analysis. *BJU Int*. 2007;99(4):786–93.

30. Swindle P, Ramadan S, Stanwell P, et al. Proton magnetic resonance spectroscopy of the central, transition and peripheral zones of the prostate: assignments and correlation with histopathology. *MAGMA*. 2008;21(6):423–34.

31. Hricak H, White S, Vigneron D, et al. Carcinoma of the prostate gland: MR imaging with pelvic phased-array coils versus integrated endorectal-pelvic phased-array coils. *Radiology*. 1994;193(3):703–9.